Eur. Phys. J. B (2020) 93: 126
https://doi.org/10.1140/epjb/e2020-100561-4

THE EUROPEAN PHYSICAL JOURNAL B

Regular Article

# Scaling behavior in measured keystroke time series from patients with Parkinson's disease

Ata Madanchi[1,2], Fatemeh Taghavi-Shahri[3], Seyed Mahmood Taghavi-Shahri[4], and Mohammed Reza Rahimi Tabar[5,6,a]

[1] Department of Physics, McGill University, H3A2T8 Montreal, Canada
[2] Montreal Institute for Learning Algorithms (MILA), H2S3H1 Montreal, Canada
[3] Department of Physics, Ferdowsi University of Mashhad, P.O. Box 1436, Mashhad, Iran
[4] Department of Epidemiology and Biostatistics, School of Public Health, Isfahan University of Medical Sciences, Isfahan, Iran
[5] Department of Physics, Sharif University of Technology, Tehran 11155-9161, Iran
[6] Institute of Physics and ForWind, Carl von Ossietzky University, 26111 Oldenburg, Germany

Received 16 November 2019 / Received in final form 21 February 2020
Published online 1 July 2020


**Abstract.** Parkinson has remained as one of the most difficult diseases to diagnose, as there are no biomarkers to be measured, and this requires one patient to do neurological and physical examinations. As Parkinson is a progressive disease, accurate detection of its symptoms is a crucial factor for therapeutic reasons. In this study, we perform Multifractal Detrended Fluctuation Analysis (MFDFA) on measured keystroke time series for three different categories of subjects: healthy, early-PD, and De-Novo patients. We have observed different scaling behavior in terms of multifractality of the measured time series, which can be used as a practical tool for diagnosis purposes. Additionally, the source of the multifractality has been studied which shows that in healthy and early-PD subjects, multifractality due to the long-range correlations is stronger than the influence of its probability distribution function (PDF) fatness, while in De-Novo patients, both shape of PDF and long-range correlations are contributing to observed multifractality.

## 1 Introduction

A broad range of complex time series in nature shows long-range correlations with scale-invariant behavior [1]. Statistically, these fluctuations often exhibit self-similar or intermittent behaviors and can be characterized by the multifractal spectrum [2]. A multifractal process may be interpreted as a superposition of subsets, each characterized by a given scaling exponent, and with a typical amplitude fluctuations [3]. This means that one needs different scaling exponents to describe strong intermittent and non-stationary time series. Although the multifractality phenomenon in the time series is not fully understood, the multifractal characterization is useful for modeling and reconstruction of time series. Characterization of complex systems based on the observed scaling behavior is the most important application of such analyses [3].

Long-range correlations are studied by scaling laws and scaling exponents classify the underlying process. According to the Wiener-Khinchin theorem, the two-point correlation function $\langle x(t+\tau)\cdot x(t)\rangle$ is directly related to the power spectrum by a Fourier transform. The correlation function is the linear regression in the $(x(t+\tau), x(t))$ plane, and it is therefore known as a linear quantity in the characterization of a given time series. Generally, one needs to analyze higher-order (non-linear) statistical properties to fully characterize a given complex time series. Let $\{x(t)\}$ be a given time series and consider its increment over a certain time lag (scale) $\tau$, which is defined as $\Delta x(\tau) = x(t+\tau) - x(t)$. We denote structure function $S(q,\tau)$ as the q-order absolute moment of $\Delta x(\tau)$, i.e.,

$$S(q,\tau) = \langle |\Delta x(\tau)|^q \rangle. \tag{1}$$

A process is called scale invariant if the absolute moment $S(q,\tau)$ has a power-law behavior in a certain range of $\tau$ [3–5]. Let us call $\xi_q$ the exponent of the power law, i.e

$$S(q,\tau) \simeq C_q \tau^{\xi_q} \tag{2}$$

where $C_q$ is a prefactor. Here $x(t)$ is called *monofractal* (or linear) if $\xi_q$ is a linear function of $q$, and *multifractal* (non-linear) if $\xi_q$ is non-linear with respect to $q$. Multifractality has been introduced in the context of fully developed turbulence in order to describe the spatial fluctuations of the fluid velocity at very high Reynolds number [2]. In the recent years multifractal analysis has successfully

[a] e-mail: mohammed.r.rahimi.tabar@uni-oldenburg.de

been applied to study the scaling properties in variety phenomena from correlation properties of coding and non-coding DNA sequences, financial time series to analysis of biomedical signals [6–32].

Among different methods for investigating the multifractal structure of the non- stationary time series, there are two more known applicable methods to detect the multifractal scaling exponents: the first one is the Wavelet Transform Modulus Maxima (WTMM) method which is based on the wavelet transformation [33–37]. It involves tracing the maxima line in the transformed signal over all scales. The second one is the Multifractal detrended fluctuation analysis (MFDFA), which is based on a generalization of the usual detrended fluctuation analysis (DFA) method [38–40]. MFDFA is the widely used technique, and it can reliably determine the multifractal spectrum and multifractal scaling behavior of the time series.

During the last decade, several studies suggest that changes in multifractality of biomedical signals can be differentiated between healthy and pathological conditions. In this paper, we use the MFDFA method to investigate the multifractality and scale-invariant properties of the measured keystroke time series from patients with Parkinson's disease (PD) which is a slowly progressing neural degenerative disease. Parkinson is the most common form of disorders in motor systems in the body. By studying a given rhythmic task to these patients, one can find out the abnormal patterns of their behavior. The Parkinson persists over a long period (chronic), and symptoms grow worse over time (progressive). The scaling analysis approaches can be integrated into many other statistical methods and machine learning techniques to enhance the accuracy of Parkinson's diagnosis [41–43]. The paper is organized as follows. In Section 2, we described the data used in this analysis. In Section 3, we briefly review the MFDFA method to study the multifractality of the time series. In Section 4, we present and discuss the results.

## 2 Description of data

The neuroQWERTY MIT-CSXPD database which we used in this analysis, contains finger-tapping recorded in routine interaction with computer keyboards collected from subjects with and without Parkinson's disease [41–43]. It is shown such interaction can be used as an indicator of the motor signs in the early stages of Parkinson's disease. The data include the key hold time, the time required to press and release a key during the regular use of computer keyboard without any change in hardware.

The dataset used in this study consists of 18 early Parkinson's disease (PD) cases and 24 De-Novo PDs cases, i.e. newly diagnosed, drug-naive patients, and 30 healthy subjects. The early-PD cases were the cases with less than 5 years from the diagnostics of PD, and the De-Novo cases were the cases with the new diagnostic of PD, and healthy subjects were subjects without any symptoms of PD. The subjects of early PD dataset examined once, but the subjects of the De-Novo dataset were examined twice in two visits with 7 to 30 days intervals. The data source is a series of hold times, the time between pressing and releasing a key on a laptop keyboard. All subjects have been reported that they use a computer, desktop, or laptop, with at least thirty minutes of use on a daily basis. A typing activity was done by all subject where the text of typing activity is randomly selected for each subject, but the system that monitored typing activity was identical. The sequence of keyboard key down times during the typing activity was recorded for each subject. Hence, a time series of key down times were provided for each subject where the length of these time series corresponded to the length of the text that subjects typed during their typing activities. More detail about neuroQWERTY dataset can be found in [41–43]. In Figure 1 three typical keystroke time (time between pushing and releasing each key) is plotted versus $N$ (data points) for each subject. The length of the time series are varied from $N \approx 1000$ to 2500 depends on the experiment.

## 3 Methods of analysis

In this section, we briefly review two standard methods, i.e. correlation function and MF-DFA to investigate the scaling and multifractal properties of stochastic processes. Also, we describe the surrogating of time series by shuffle, random-phase and rank-wised methods which are used to detect the source of multifractality.

### 3.1 Long and short range correlations

For the given time series $x(t_i) \equiv x(i)$ for $\{i = 1, \cdots, N\}$, we define the mean of $x$ series as, $< x >= \frac{1}{N}\sum_{i=1}^{N} x_i$. The anomaly of the time series, $\bar{x}_i$, is defined as $\bar{x}_i = x_i - \langle x \rangle$. For a stationary data the correlation function defined as $C(s)$ given by, $C(s) = \langle \bar{x}_i \bar{x}_{i+s} \rangle = \frac{1}{N-s}\sum_{i=1}^{N-s} \bar{x}_i \bar{x}_{i+s}$. If $x(i)$ is uncorrelated, $C(s)$ for $s > 0$ will be zero. The short-range correlations declining exponentially [44–47], $C(s) \sim \exp(-\frac{s}{s_d})$, with a specific decay time scale $s_d$. For long-range correlation, $C(s)$ behaves power-law, $C(s) \sim s^{-\gamma}$ with the exponent $0 < \gamma < 1$. The long-range correlation is studied by the well-known Hurst exponent $H = 1 - \gamma/2$ [44–47], and its power spectra can be characterized by $S(\omega) \sim \omega^{-\beta}$. Here $\omega$ is angular frequency and power spectrum exponent is given by $\beta = 2H - 1$ for stationary data set. In practice, almost all experimental data sets are affected by some non-stationarities like trends, which have to be well distinguished from the intrinsic fluctuations of the process in order to find the correct scaling behavior of the fluctuations. Nondetrending methods, like correlation function, work well if the records are long and do not involve trends. However, if trends are present in the data, they will provide wrong results. Detrended fluctuation analysis (DFA) is a well-established method for determining the scaling behavior of noisy data in the presence of trends without knowing the trend's origin and shape a priori.

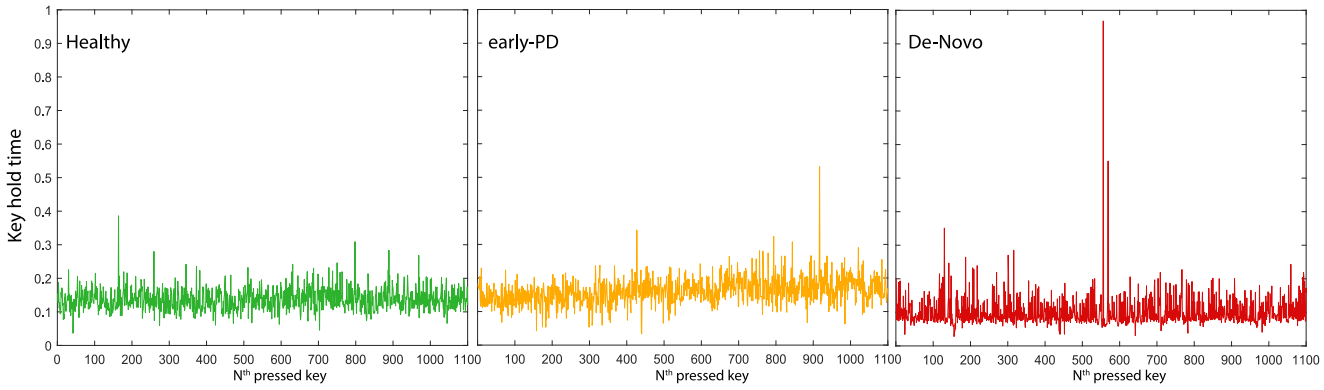


**Fig. 1.** Segments of the time series of keystroke for a healthy, early-PD, and a De-Novo subject.

### 3.2 Detrended and multifractal detrended fluctuation analyses

Detrended fluctuation analysis (DFA) and Multifractal detrended fluctuation analysis (MFDFA) can used for studying scaling properties and detecting long-range correlations in general non-stationary time series. More detail about these algorithms can be found in [38–40] and [48–52]. In MFDFA approach, the time series (with the length of $N$) is divided into the $N_s = \frac{N}{s}$ segments, and each segment is detrended using a polynomial function. The generalized fluctuation function $F_q(s)$, defined as follows has scaling behavior with exponent $h(q)$,

$$F_q(s) = \{\frac{1}{2N_s}\sum_{v=1}^{2N_s}[F_s^2(v)]^{\frac{q}{2}}\}^{\frac{1}{q}} \sim s^{h(q)} \quad . \qquad (3)$$

The case $q = 2$ corresponds to the DFA. For $q = 2$, $F_2(s)$ behaves as a power law regarding the scale $s$, with a power law exponent, $h(2)$ known as Hurst exponent. In MFDFA, $h(q)$ is called the generalized Hurst exponent. The MFDFA approach can distinguish between small and large fluctuation statistics for negative and positive values of $q$. For stationary processes $H = h(q = 2) < 1.0$, is the Hurst exponent, and for non-stationary processes, one can show $h(q = 2) > 1.0$ [27,30]. In this case the Hurst exponent can be calculated as $H = h(q = 2) - 1$ [39,45,51]. The Hurst exponent $H = 0.5$, indicates that the time series are uncorrelated; $0 < H < 0.5$ implies short-term anti-persistence and $0.5 < H < 1$ implies long-term persistence [26]. For non-stationary time series, the correlation exponent and power spectrum scaling are $\gamma = -2H$ and $\beta = 2H + 1$, respectively [6,45,47]. The function $h(q)$ for positive values of $q$ represents the scaling behavior of the segments with large fluctuations. On the contrary, for negative values of $q$ small variances of $F_s^2(v)$ in equation (11) will dominate the average $F_q(s)$ in equation (3) and $h(q)$ describes the scaling behavior of the segments with small fluctuations [37].

There is a direct dependence between the generalized Hurst exponent MF-DFA and the classical multifractal scaling exponents $\tau(q)$ (Renyi exponent) as, $\tau(q) = qh(q) - 1$ [37]. A monofractal time series with long-range correlation is characterized by a single Hurst exponent with no dependency of $h(q)$ on $q$. However, a multifractal time series has several Hurst exponents with dependence of $h(q)$ on $q$. The multifractal dimensions, $D(q)$, is defined as $D(q) \equiv \frac{\tau(q)}{q-1} = \frac{qh(q)-1}{q-1}$. Legendre transformation from $\tau(q)$ to $f(\alpha)$ is known as singularity spectrum, which is given by [39,44], $f(\alpha) = q\alpha - \tau^{'}(q)$ with $\alpha = \tau^{'}(q)$, where $\alpha$ is the singularity strength or Hölder exponent and $\tau^{'}(q) = \frac{d}{dq}\tau(q)$. The spectrum $f(\alpha)$ will be $f(\alpha) = q[\alpha - h(q)] + 1$ with $\alpha = h(q) + qh^{'}(q)$. The alternative way to address the multifractality is the Hölder exponent. In the multifractal case, the different parts of the structure are characterized by different values of $\alpha$, leading to the existence of the spectrum $f(\alpha)$.

### 3.3 The shuffled, rank-wise and random-phase surrogated data

There are two main reasons for multifractality of given time series,

1. Existence of wide or fat-tail probability density function (PDF).
2. Existence linear and non-linear correlations in the time series.

To understand the origin of multifractality, one can explore each of these features separately [26,53–55]. For destroying all types of correlations, we need to shuffle data. In this way, we will study the influence of just the shape of the distribution function of the data set on multifractality. For detecting effects of fat-tailed PDF, by keeping *linear* correlation, we can change any distribution of given time series to a gaussian distribution with a so-called Random-Phase (RP) data surrogating. This is done simply by calculating the Fourier transform of time series and multiplying them by random phases with uniform distribution [53]. Another method which exchanges PDF of time series by a Gaussian distribution, is known as Rank-Wised (RW) surrogation, that keeps *linear* and *non-linear* correlations but non-gaussian distributional effect are removed [26]. In this way to eliminate the dependence of observed multifractality on the fat-tailed distribution,

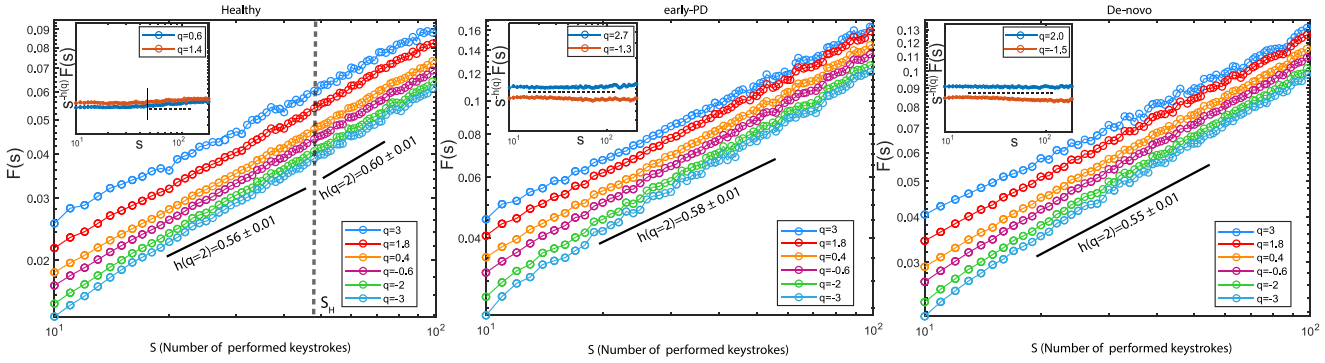


**Fig. 2.** Plot of $F_q(s)$ vs. $s$ for healthy subjects as well as for early-PD and De-Novo subjects without taking any medicine, averaged over all the patients studied in each category. The slopes of $F(s)$ for $q = 2$ have been shown as a reference. For healthy subjects a crossover is observed at time scale $S \approx 48$. In order to observe this crossover clearly, we have plotted the compensated fluctuation functions $s^{-h(q)}F(s)$ in the insets with small offsets.

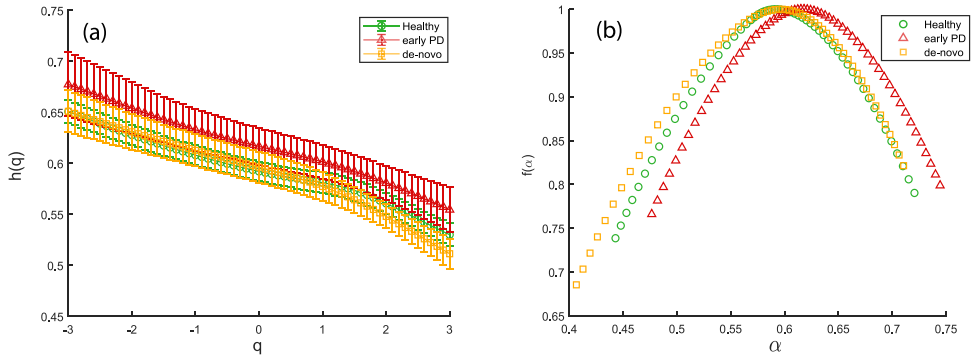


**Fig. 3.** Comparison of the estimated exponents $h(q)$, $\tau(q)$ and singularity spectrum $f(\alpha)$ for healthy subjects and early-PD and De-Novo subjects. The demonstrated curves correspond to the scales smaller than the crossover time scale ($s < S_H$) for healthy subjects. (a) Shows lower $h(q)$ for healthy and De-novo subjects. Also, the degree of multifractality for each case is compared in (b).

we have first ranked the $N$ values of time series in the original data, and then exchanged them rank wise by a set of $N$ numbers from a Gaussian distribution [54].

## 4 Results

### 4.1 Results of MFDFA for healthy subjects and patients who are suffering from Parkinson's disease

To investigate the multifractal properties of control subjects and PD patients, one can compute $F_q(s)$ as the function of $s$. Figure 2 shows the log-log plot of $F_q(s)$ by MFDFA (order 1) for healthy subjects as well as for early-PD and De-Novo patients. For healthy subjects, a crossover has been observed at time scale $S_H \approx 48$. For early-PD and De-novo subjects, no crossover is present. Figure 3 compares the $h(q)$ and $f(\alpha)$ of early-PD and De-Novo subjects with the results obtained for healthy subjects below time scale $S_H$, and Figure 4 demonstrates the same parameters but with considering the scales above $S_H$ for healthy subjects. The dependency of $h(q)$ on $q$, demonstrate the multifractality of keystroke data sets in all cases. Having $h(q) < 1.0$, put the keystroke time series in the class of stationary processes.

By comparing the width of the singularity spectrum $\Delta\alpha$, the degree of multifractality can be measured. In short time scales (below crossover $S_H$), healthy subjects show higher multifractality with $\Delta\alpha = 0.29 \pm 0.02$ compared to the large scales with $\Delta\alpha = 0.16 \pm 0.02$. The PD patients who treated with medicine (early-PD) have $\Delta\alpha = 0.29 \pm 0.05$ comparable with De-Novo subjects with $\Delta\alpha = 0.31 \pm 0.05$.

As a result, we can conclude that healthy subjects have stronger multifractality in shorter time scales. At long time scales, however, healthy subjects have monofractal behavior. Patients who are suffering from Parkinson demonstrate more complex behavior which leads to a little higher multifractality. Table 1 includes the estimated $\Delta\alpha$, averaged over all the patients in each categories. Therefore, degree of multifractality, i.e. $\Delta\alpha$, can be considered as a potential indicator of patients who are suffering from Parkinson's disease. The higher complexity of finger tapping time series for PD sufferers is according to our expectations, due to the lack of ability of PD patients to keep the long term rhythms, and also the higher intermittency of the signals as a result of tremors. Dutta et al. have also investigated multifractality of gait rhythm obtained from heel strikes and the measured stride interval time series [56] and have measured higher multifractality for

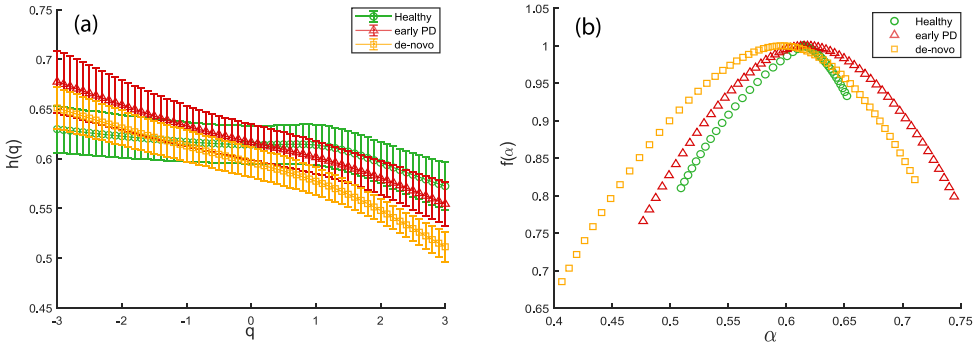


**Fig. 4.** Comparison of the exponents $h(q)$, $\tau(q)$ and singularity spectrum $f(\alpha)$ between healthy subjects (large time scales) and early-PD and De-Novo subjects. The demonstrated curves are corresponded to the scales longer than the crossover ($s > S_H$) for healthy subjects.

normal subjects. Other similar studies, have also used the multifractal analysis to quantify the statistics of neuro-degenerative diseases [57,58].

### 4.2 Origin of the multifractality

By surrogating data using shuffling, random phase, and rank-wised methods, the source of multifractality can be understood. To determine the type of multifractality, one can compare the fluctuation function for the original time series, $F_q(s)$, with the fluctuation function for the shuffled, random phase and rank-wise surrogated data, i.e., $F_q^{\text{shuf}}(s)$, $F_q^{\text{RP-sur}}(s)$ and $F_q^{\text{RW-sur}}(s)$, respectively. By considering their ratio we have:

$$F_q(s)/F_q^{\text{shuf}}(s) = s^{h(q)-h_{\text{shuf}}(q)} = s^{h_{\text{corr}}(q)}, \tag{4}$$

$$F_q(s)/F_q^{\text{RP-sur}}(s) = s^{h(q)-h_{\text{RP-sur}}(q)} = s^{h_{\text{PDF-RP}}(q)} \tag{5}$$

$$F_q(s)/F_q^{\text{RW-sur}}(s) = s^{h(q)-h_{\text{RW-sur}}(q)} = s^{h_{\text{PDF-RW}}(q)}. \tag{6}$$

Multifractality of a time series can be attributed to three causes. The first is a broad probability density function (PDF) of the time series, the second is a linear correlation inherent in the data, and the third is the presence of mixed linear and non-linear correlations. The result of surrogated $h(q)$, and $f(\alpha)$ for healthy subjects are shown in Figure 5, and for early-PD and De-Novo patients depicted in Figure 6.

In all type of subjects, the exponents $h_{\text{corr}}(q)$, $h_{\text{PDF-RP}}(q)$ and $h_{\text{PDF-RW}}(q)$ have dependency on $q$, revealing that the nature of multifractality in keystroke time series are due to broadness of PDF and long-range correlations. Also in RP-surrogated data, $h_{\text{PDF-RW}}(q)$ has the least deviation from $h_{\text{origin}}(q)$ for all three type of subjects, claiming that contribution of linear and non-linear correlations are stronger than fatness of PDF. More could be understood, by comparing $h_{\text{PDF-RP}}(q)$ and $h_{\text{corr}}(q)$. The deviation of $h_{\text{RP-sur}}(q)$ and $h_{\text{shuf}}(q)$ from $h(q)$ is determined by using a $\chi^2$ test, for instance,

$$\chi^2 = \frac{1}{N}\sum_{i=1}^{N}\frac{[h(q_i) - h_s(q_i)]^2}{\sigma(q_i)^2 + \sigma_s(q_i)^2}. \tag{7}$$

**Table 1.** Estimated mean value of $\Delta\alpha$ for healthy, early-PD, and De-Novo subjects. In the last row, the mean of $\Delta\alpha$ values for healthy and early-PD subjects are compared to the $\Delta\alpha$ value obtained for De-Novo subjects.

| Subject | Healthy | early-PD | De-Novo |
|---|---|---|---|
| $\Delta\alpha_{s<s_c}$ | $0.29 \pm 0.02$ | $n/a$ | $n/a$ |
| $\Delta\alpha_{s>s_c}$ | $0.16 \pm 0.02$ | $n/a$ | $n/a$ |
| $\Delta\alpha_{s(mean)}$ | $0.22 \pm 0.02$ | $0.29 \pm 0.05$ | $0.31 \pm 0.05$ |

Here $h_s(q)$ is the Hurst exponent of the desired surrogation, which in our case is shuffled, RP-surrogation and RW-surrogation. As $h_{\text{PDF-RW}}(q)$ has the least deviation, here we only compare the obtained $\chi^2$ test values for RW-Surrogation and shuffle methods. For healthy subjects and in short time scales, $s < S_H$, $\chi^2_{\text{H,shuf}} = 9.20$ and $\chi^2_{\text{H,RP-sur}} = 6.21$, and in large time scales, $s > S_H$, $\chi^2_{\text{H,shuf}} = 20.63$ and $\chi^2_{\text{H,RP-sur}} = 4.66$. While the contribution of PDF and correlations are comparable in short scales, their difference is more pronounced in longer scales. The $\chi^2$ test values for early-PD subjects are $\chi^2_{\text{P,shuf}} = 12.03$ and $\chi^2_{\text{P,RP-sur}} = 2.27$. For De-Novo subjects $\chi^2_{\text{D,shuf}} = 6.70$ and $\chi^2_{\text{D,RP-sur}} = 5.14$.

Although the degree of multifractality, $\Delta\alpha$ for early-PD and De-Novo subjects are shown to be in the same level, for De-Novo patients, both PDF fatness and long-range correlations are equivalently important. One can conclude that for patients without getting treatment (De-Novo subjects), the probability of rare events have a high impact on their multifractal behavior, while in early-PD cases medication has made them to perform keystroke similar to healthy subjects as the main source of the multifractality for early-PD and healthy subjects is the long-range correlations. The numerical values of $\chi^2$-test are summarized in Table 2. Additionally, the $\Delta\alpha$ values of surrogated data are reported in Table 3.

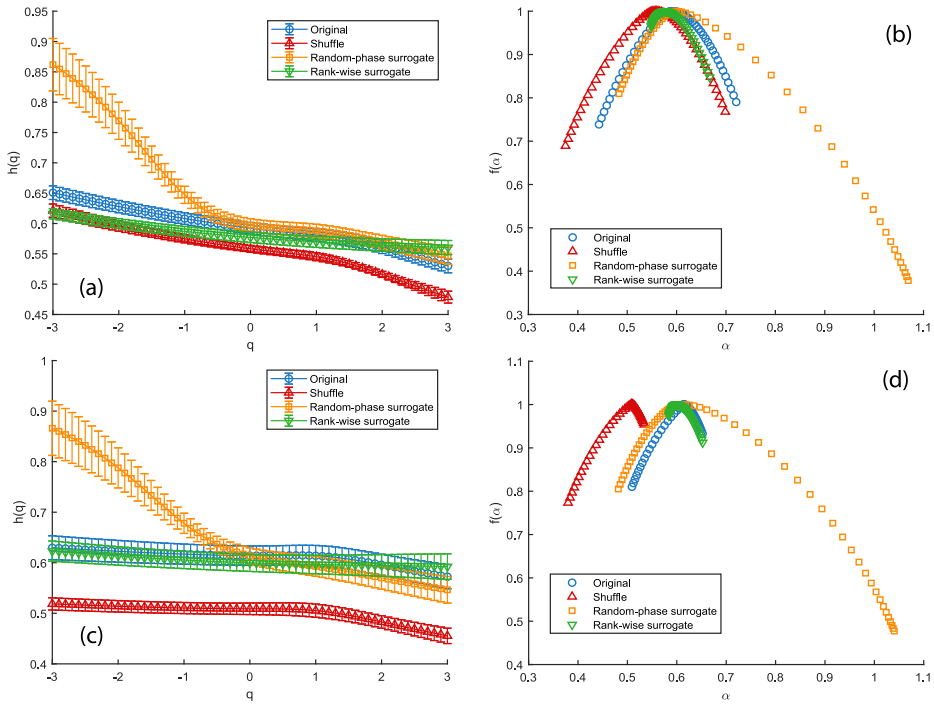


**Fig. 5.** The exponent $h(q)$, and $f(\alpha)$ for original, shuffled, random-phase (RP) surrogated data and rank-wise (RW) surrogated data sets of healthy subjects. (a) and (b) are for scales $s < S_H$, and (c) and (d) are for $s > S_H$.

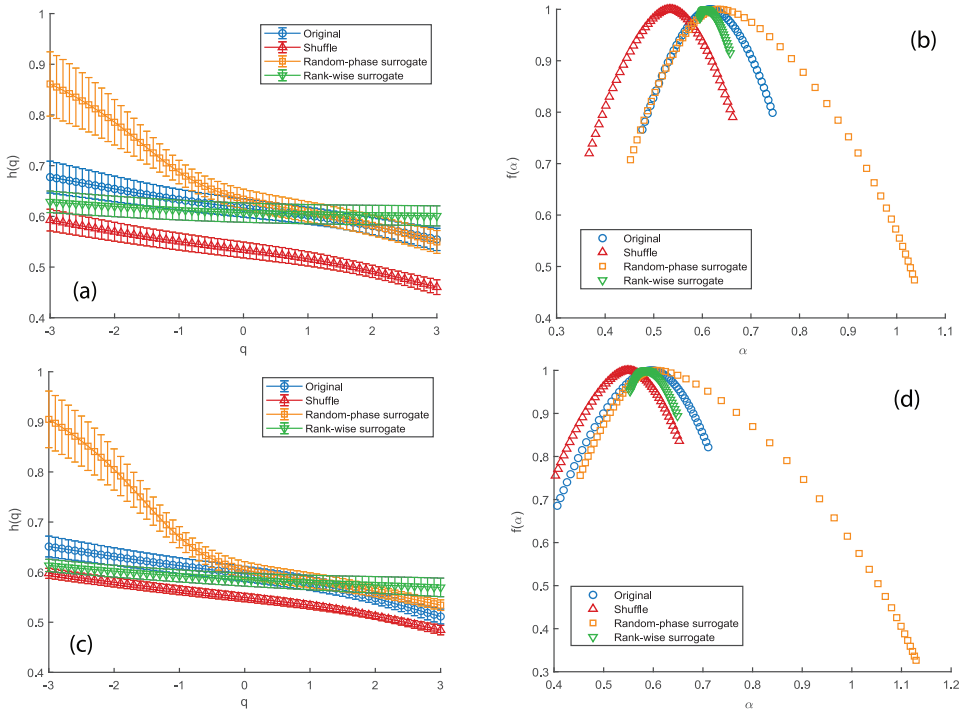


**Fig. 6.** The exponent $h(q)$, and $f(\alpha)$ for original, shuffled, RP-surrogated and RW-surrogated data sets of early-PD subjects are demonstrated in (a) and (b) and De-Novo subjects are reported in (c) and (d).

In summary, in this paper, we have performed MFDFA analysis on keystroke data sets of healthy, early-PD, and De-Novo subjects. We have found that the degree of multifractality can be taken as a measure to distinguish patients suffering from Parkinson's disease in comparison with healthy subjects. The nature of multifractality has been investigated in all three groups, showing the importance of non-linear correlation and shape of

**Table 2.** The $\chi^2$ values of RP-surrogated, RW-surrogated and shuffled time series for healthy, early-PD, and De-Novo subjects. In the last two rows, the mean values of calculated $\chi^2$ for healthy and early-PD subjects are compared to the their values for De-Novo subjects as no crossover is found for them.

| Subject | Healthy | early-PD | De-Novo |
|---|---|---|---|
| $\chi^2_{\text{shuf},s<s_c}$ | 9.20 | $n/a$ | $n/a$ |
| $\chi^2_{\text{RP-sur},s<s_c}$ | 6.21 | $n/a$ | $n/a$ |
| $\chi^2_{\text{RW-sur},s<s_c}$ | 2.35 | $n/a$ | $n/a$ |
| $\chi^2_{\text{shuf},s>s_c}$ | 20.63 | $n/a$ | $n/a$ |
| $\chi^2_{\text{RP-sur},s>s_c}$ | 4.66 | $n/a$ | $n/a$ |
| $\chi^2_{\text{RW-sur},s>s_c}$ | 0.19 | $n/a$ | $n/a$ |
| $\chi^2_{\text{shuf},s(mean)}$ | 14.91 | 12.03 | 6.70 |
| $\chi^2_{\text{RP-sur},s(mean)}$ | 5.43 | 2.27 | 5.14 |
| $\chi^2_{\text{RW-sur},s(mean)}$ | 1.27 | 0.75 | 1.51 |

**Table 3.** The $\Delta\alpha$ values of RP-surrogated, RW-surrogated and shuffled time series for healthy, early-PD, and De-Novo subjects. In the last two rows, the mean value of calculated $\chi^2$ for healthy and early-PD subjects are compared to the their values for De-Novo subjects as no crossover is found for them.

| Subject | Healthy | early-PD | De-Novo |
|---|---|---|---|
| $\Delta\alpha_{\text{shuf},s<s_c}$ | $0.33 \pm 0.03$ | $n/a$ | $n/a$ |
| $\Delta\alpha_{\text{RP-sur},s<s_c}$ | $0.61 \pm 0.06$ | $n/a$ | $n/a$ |
| $\Delta\alpha_{\text{RW-sur},s<s_c}$ | $0.11 \pm 0.02$ | $n/a$ | $n/a$ |
| $\Delta\alpha_{\text{shuf},s>s_c}$ | $0.22 \pm 0.03$ | $n/a$ | $n/a$ |
| $\Delta\alpha_{\text{RP-sur},s>s_c}$ | $0.64 \pm 0.08$ | $n/a$ | $n/a$ |
| $\Delta\alpha_{\text{RW-sur},s>s_c}$ | $0.07 \pm 0.03$ | $n/a$ | $n/a$ |
| $\Delta\alpha_{\text{shuf},s(mean)}$ | $0.27 \pm 0.03$ | $0.30 \pm 0.05$ | $0.25 \pm 0.03$ |
| $\Delta\alpha_{\text{RP-sur},s(mean)}$ | $0.62 \pm 0.07$ | $0.61 \pm 0.10$ | $0.68 \pm 0.08$ |
| $\Delta\alpha_{\text{RW-sur},s(mean)}$ | $0.09 \pm 0.03$ | $0.06 \pm 0.03$ | $0.10 \pm 0.02$ |

probability distribution functions in multifractal behavior of keystroke time series. Our results characterize the scaling behavior of keystroke data sets for aforementioned subjects at different time scales.

## Author contribution statement

M. R. R. T. and F. T. S. designed the study. A. M., F. T. S. and S. M. T. S. wrote the manuscript. Computer codes were written by A. M. All authors analysed the data and reviewed the manuscript.



## References

1. J.W. Kantelhardt, *Mathematics of Complexity and Dynamical Systems*, edited by R.A. Meyers (Springer, New York, 2012), pp. 463-487
2. U. Frisch, *Turbulence, The Legacy of A. N. Kolmogorov* (Cambridge University Press, Cambridge, England, 1995)
3. M.R. Rahimi Tabar, *Analysis and Data-Based Reconstruction of Complex Nonlinear Dynamical Systems: Using the Methods of Stochastic Processes* (Springer, Switzerland, 2019)
4. R. Friedrich, J. Peinke, M. Sahimi, M.R. Rahimi Tabar, Phys. Rep. **506**, 87 (2011)
5. J. Peinke, M.R. Rahimi Tabar, M. Wächter, Ann. Rev. Condens. Matter Phys. **10**, 110 (2019)
6. C. Peng, S. Buldyrev, M. Simons, H. Stanley, A. Goldberger, Phys. Rev. E **49**, 1685 (1994)
7. Z. Jiang, W. Xie , W. Zhou, D. Sornette, Rep. Prog. Phys. **82**, 12 (2019)
8. P. Baranowski, J. Krzyszczak, C. Slawinski, H. Hoffmann, J. Kozyra, A. Nierobca, K. Siwek, A. Gluza, Clim. Res. **65**, 39 (2015)
9. M. Laib, J. Golay, L. Telesca, M. Kanevski, Chaos Solitons Fractals **109**, 118 (2018)
10. R. Morales, T.D. Matteo, R. Gramatica, T. Aste, Physica A **391**, 3180 (2012)
11. J. Barunik, T. Aste, T.D. Matteo, R. Liu, Physica A **391**, 4234 (2012)
12. R. Morales, T.D. Matteo, T. Aste, Physica A **392**, 6470 (2013)
13. A.Y. Schumann, J.W. Kantelhardt, Physica A **390**, 14 (2011).
14. J. Ludescher, M.I. Bogachev, J.W. Kantelhardt, A.Y. Schumann, A. Bunde, Physica A **390**, 2480 (2011).
15. X. Zhang, H. Liu, Y. Zhao, X. Zhang, Physica A **531**, 121790 (2019)
16. J. Wang, P. Shang, X. Cui, Phys. Rev. E **89**, 032916 (2014)
17. S. Blesic, S. Milosevic, D. Stratimirovic, M. Ljubisavljevic, Physica A **268**, 275 (1999)
18. S. Bahar, J.W. Kantelhardt, A. Neiman, H.H.A. Rego, D.F. Russell, L. Wilkens, A. Bunde, F. Moss, Europhys. Lett. **56**, 454 (2001)
19. S. Shadkhoo, F. Ghanbarnejad, G.R. Jafari, M.R. Rahimi Tabar, Cent. Eur. J. Phys. **7**, 620 (2009)
20. M.S. Movahed, F. Ghasemi, S. Rahvar, M.R. Rahimi Tabar, Phys. Rev. E **84**, 021103 (2011)
21. R. Lopes, N. Betrouni, Med. Image Anal. **13**, 634 (2009)
22. M R. Rahimi Tabar, et al., Comput. Sci. Eng. **8**, 54 (2006)
23. L.F. Marton , S.T. Brassai, L. Bako, L. Losonczi, Procedia Technol. **12**, 125 (2014)
24. Y. Wu, S. Krishnan, Engineering **18**, 150 (2010)
25. M.R. Rahimi Tabar, M. Anvari, G. Lohmann, D. Heinemann, M. Wächter, P. Milan, E. Lorenz, J. Peinke, Eur. Phys. J. Special Topics **223**, 2637 (2014)
26. A. Madanchi, M. Absalan, G. Lohmann, M. Anvari, M.R. Rahimi Tabar, Solar Energy **144**, 1 (2017)
27. M.S. Movahed, G.R. Jafari, F. Ghasemi, S. Rahvar, M.R. Rahimi Tabar, J. Stat. Mech. **02**, P02003 (2006)
28. Z. Fayyaz, M. Bahdorian, J. Doostmohammadi, V. Davoodnia, S. Khodadadian, R. Lashgari, J. Neurosci. Methods **312**, 84 (2019)
29. P. Shang, Y. Lu, S. Kamae, Chaos Solitons Fractals **36**, 82 (2008)
30. A. Facchini, S. Wimberger, A. Tomadin, Physica A **376**, 266 (2007)
31. A.K. Maity, R. Pratihar, A. Mitra, S. Dey, V. Agrawal, S. Sanyal, A. Banerjee, R. Sengupta, D. Ghosh, Chaos Solitons Fractals **81**, 52 (2015)

32. L. Telesca, M. Lovallo, M. Kanevski, Appl. Energy **162** 1052 (2016)
33. J.F. Muzy, E. Bacry, A. Arneodo, Int. J. Bifurc. Chaos **4**, 245 (1994)
34. A. Arneodo, E. Bacry, P.V. Graves, J.F. Muzy, Phys. Rev. Lett. **74**, 3293 (1995)
35. P.Ch. Ivanov, L.A.N. Amaral, A.L. Goldberger, S. Havlin, M.G. Rosenblum, Z.R. Struzik, H.E. Stanley, Nature **399**, 461 (1999)
36. L.A.N. Amaral, P. Ch. Ivanov, N. Aoyagi, I. Hidaka, S. Tomono, A.L. Goldberger, H.E. Stanley, Y. Yamamoto, Phys. Rev. Lett. **86**, 6026 (2001)
37. A. Silchenko, C.K. Hu, Phys. Rev. E **63**, 041105 (2001)
38. J.W. Kantelhardt, S.A. Zschiegner, E. Koscielny-Bunde, S. Havlin, A. Bunde, H.E. Stanley, Physica A **316**, 87 (2002)
39. A. Goldberger, L. Amaral, L. Glass, J. Hausdorff, P. Ivanov, R. Mark, J. Mietus, G. Moody, C.K. Peng, H.E. Stanley, Circulation **101**, 215 (2000)
40. E.A.F. Ihlen, Front. Physiol. **3**, 141 (2012)
41. L. Giancardo, A. Sánchez-Ferro, T. Arroyo-Gallego, I. Butterworth, C.S. Mendoza, P. Montero, M. Matarazzo, J.A. Obeso, M.L. Gray, R.S.J. Estépar, Sci. Rep. **6**, 34468 (2016)
42. B. Lan, J.H.W. Yeo, PLoS One **14**, 6 (2019)
43. W.R. Adams, PLoS One **12**, e0188226 (2017)
44. J. Feder, *Fractals* (Plenum Press, New York, 1988)
45. H.O. Peitgen, H. Jurgens, D. Saupe, *Chaos and Fractals* (Springer-Verlag, New York, 1992)
46. S.M. Ossadnik, S.B. Buldyrev, A.L. Goldberger, S. Havlin, R.N. Mantegna, C.K. Peng, M. Simons, H.E. Stanley, Biophys. J. **67**, 64 (1994)
47. J.W. Kantelhardt, Fractal and multifractal time series, in *Mathematics of Complexity and Dynamical Systems*, edited by R.A. Meyers (Springer, New York, 2011), pp. 463–487
48. A. Eke, P. Herman, L. Kocsis, L.R. Kozak, Physiol. Meas. **23**, R1-38 (2002)
49. M.S. Taqqu, V. Teverovsky, W. Willinger, Fractals **3**, 785 (1995)
50. K. Hu, P. Ch. Ivanov, Z. Chen, P. Carpena, H.E. Stanley, Phys. Rev. E **64**, 011114 (2001)
51. Z. Chen, P. Ch. Ivanov, K. Hu, H.E. Stanley, Phys. Rev. E **65**, 041107 (2002)
52. A. Bunde, S. Havlin, J.W. Kantelhardt, T. Penzel, J.H. Peter, K. Voigt, Phys. Rev. Lett. **85**, 3736 (2000)
53. P. Manshour, M.R. Rahimi Tabar, J. Peinke, J. Stat. Mech. **8**, P08031 (2015)
54. T. Schreiber, A. Schmitz, Phys. Rev. Lett. **77**, 635 (1996)
55. M.I. Bogachev, J.F. Eichner, A. Bunde, Phys. Rev. Lett. **99**, 240601 (2007)
56. S. Dutta, D. Ghosh, S. Chatterjee, Front. Physiol. **4**, 274 (2013)
57. N. Scafetta, R. Moon, B.J. West, Complexity **12**, 12 (2007)
58. D. Ghosh, S. Samanta, S. Chakraborty, *Multifractals and Chronic Diseases of the Central Nervous System* (Springer, Berlin, 2019), pp. 117–147